**EMITTER International Journal of Engineering Technology**
Vol. 12, No. 2, December 2024, pp. 196~212
DOI : 10.24003/emitter.v12i2.904

# Implementation of Portable Ultrasound for Heart Disease Detection Using Cloud Computing-Based Machine Learning

Riyanto Sigit[1], Rika Rokhana[2], Setiawardhana[1], Taufiq Hidayat[3], Anwar[4], Jovan Josafat Jaenputra[1]

[1]Department of Informatic and Computer Engineering, Politeknik Elektronika Negeri Surabaya, Surabaya, East Java, Indonesia
[2]Department of Electrical Engineering, Politeknik Elektronika Negeri Surabaya, Surabaya, East Java, Indonesia
[3]Department of Pediatrics, Faculty of Medicine Universitas Airlangga, Surabaya, East Java, Indonesia
[4]Ministry of Manpower, Jakarta Selatan, Jakarta, Indonesia
Corresponding author: riyanto@pens.ac.id.

*Received October 3, 2024; Revised November 7, 2024; Accepted December 12, 2024*

**Abstract**

Heart disease remains one of the leading causes of death globally, including in Indonesia. Cardiovascular disease is the leading cause of death worldwide, resulting in a significant number of fatalities. In Indonesia, access to specialized heart examination services is limited, requiring patients to visit large hospitals equipped with specialized facilities. Echocardiographic examinations using ultrasound can measure various heart parameters, such as hemodynamics, heart mass, and myocardial deformation. Portable ultrasound devices have emerged, enabling flexible and effective heart examinations. These devices capture video data of the patient's heart condition. The data undergoes image preprocessing involving median filtering, high-boost filtering, morphological operations, thresholding, and Canny filtering. Segmentation is performed using region filters, collinear filters, and triangle equations. Tracking utilizes the Optical Flow Lucas-Kanade method, and feature extraction employs Euclidean distance and trigonometric equations. The classification stage uses Support Vector Machine (SVM). Video data is transmitted via a mobile application to the cloud, where all stages from preprocessing to classification are conducted on cloud servers. The classification results are then sent back to the mobile application. The proposed model achieved an accuracy rate of 86% with a standard deviation of 0.09, indicating that the detection system performs effectively.

**Keywords**: Echocardiography, Ultrasound Portable, Cloud Computing, Image Processing

## 1. INTRODUCTION

Cardiovascular disease is the leading cause of death worldwide, resulting in a significant number of fatalities. In 2021 alone, this disease caused 20.5

Copyright © 2024 EMITTER International Journal of Engineering Technology - Published by PENS

million deaths, accounting for about one-third of all global deaths [1]. Slow handling and limited examination facilities are key reasons why heart disease can become fatal and lead to death. Therefore, a highly mobile tool is needed to detect a patient's heart condition, enabling timely and appropriate treatment. An echocardiogram is a diagnostic method that uses high-frequency sound waves to capture images of the heart's structure and function. [2][3]. Therefore, a portable ultrasound device is needed to allow flexible examinations without requiring a hospital visit [4][5]. Currently, portable ultrasound devices have been developed in relatively small sizes and can be integrated with Android devices. Ultrasound images can be transmitted to Android devices via a wireless Wi-Fi connection linked to the ultrasound device [6]. Currently, research has enabled the display of visual data in video format, which is then sent to an embedded PC via a USB connection. This echocardiography process involves several stages of image processing: preprocessing, segmentation, tracking, feature extraction, and classification using machine learning, as detailed in previous research [7][8].

However, image processing and classification conducted on embedded PCs present challenges for portable ultrasound devices in achieving flexibility of use. Therefore, a more efficient and practical solution is to utilize cloud computing technology. Cloud computing offers flexible, scalable, and remotely accessible computing capabilities [9]. This research transitions data processing for portable ultrasound devices from embedded PCs to the cloud, covering preprocessing, segmentation, tracking, feature extraction, and classification. Echocardiography images are uploaded to the cloud for processing, with results sent back to Android devices, enabling quick access to patient heart condition data. By leveraging cloud computing, the system enhances practicality and efficiency, reduces reliance on local embedded PC capabilities, and lowers equipment costs by eliminating the need for expensive local hardware.

## 2. RELATED WORKS

Coronary Heart Disease (CHD) is the top cause of death in Indonesia. Since 2002, myocardial infarction, a type of CHD, has accounted for 13.49% of deaths, with its prevalence increasing each year [10]. Echocardiography is a primary tool used to diagnose and evaluate coronary heart disease. The article titled "Artificial Intelligence in Echocardiography: Detection, Functional Evaluation, and Disease Diagnosis" discusses the application of AI in echocardiography. The use of AI in analyzing cardiac ultrasound images can enhance disease detection by reducing reliance on the sonographer's skills and experience. Advances in mobile and wireless technology have led to significant progress in cardiovascular imaging [11]. The article "Early and Accurate Detection and Diagnosis of Heart Disease Using Intelligent Computational Models" evaluates various intelligent computational prediction systems using machine learning to identify and diagnose heart disease. This early detection

system has demonstrated the ability to identify and classify CHD with up to 90% accuracy using various machine learning algorithms [12].

The study titled "Cloud-Based Services for Biomedical Image Analysis" implements a cloud-based image analysis and processing system divided into several layers: Infrastructure as a Service (IaaS) for the NeCTAR research cloud, Platform as a Service (PaaS) for development and runtime environments, and Software as a Service (SaaS) for web-based image analysis portals. The study demonstrates that cloud-based image analysis systems offer scalable, agile, and cost-effective resources for scientists [13]. Similarly, the study "Image Cloud: Medical Image Processing as a Service for Regional Healthcare in a Hybrid Cloud Environment" builds a medical image processing system using a three-layer hybrid cloud where image processing occurs on the platform layer [14]. Another study, "Smart Cloud System with Image Processing Server in Diagnosing Brain Diseases," aimed to assist hospitals with limited resources by developing a real-time diagnostic system using the ITK library and the Simple Object Access Protocol (SOAP) web service. This system achieved an average response time of 7.0 ± 0.3 seconds from data transmission to receipt [15].

## 3. ORIGINALITY

This study introduces an innovative system that integrates echocardiography technology with portable ultrasound equipment and cloud-based data processing to accelerate and simplify the diagnosis of heart disease. This system enables doctors to perform heart examinations flexibly and effectively from any location, without the need for large hospital facilities. The main advantage of this study is the complete processing of patient heart video images in the cloud, from preprocessing to classification using Support Vector Machine (SVM). The focus is on the PSAX (Parasternal Short Axis) view. Videos captured with portable ultrasound undergo advanced image preprocessing, including median filtering, high-boost filtering, thresholding, and Canny edge detection. Segmentation is performed using region filters, collinear filters, and triangle equations, while tracking is carried out using the Lucas-Kanade Optical Flow method. Key features are extracted using Euclidean distance and trigonometric equations before being classified with SVM.

The novelty of this research lies in the full integration of echocardiography technology with portable ultrasound devices, cloud-based data processing, and mobile application delivery, which enables seamless heart disease diagnosis. Unlike existing systems that rely on local embedded PCs or partial integration, this approach combines advanced preprocessing techniques, segmentation, and feature extraction with classification using SVM entirely in the cloud. Techniques such as median filtering and Canny edge detection are used for their effectiveness in reducing noise and detecting precise edges in medical images, which are critical for accurate segmentation and feature extraction. The PSAX view is chosen for its clinical significance in providing a cross-sectional view of the heart, essential for detecting structural

abnormalities. By leveraging these methods, the system enhances diagnostic accuracy, speeds up the process with scalable cloud computing, and provides a cost-effective solution for remote heart examinations, distinguishing itself from prior work.

## 4. SYSTEM DESIGN

System design is conducted prior to the implementation stage to ensure the system operates optimally. The system diagram in Figure 1 illustrates the overall workflow of the system designed for this research. Each component of the diagram outlines the processes to be implemented, described as follows.

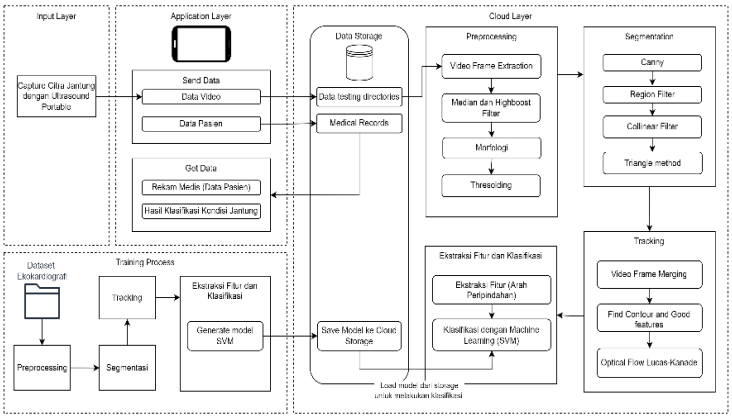


**Figure 1.** Desain Sistem

### 4.1 Dataset

The dataset collection was conducted at Jemursari Islamic Hospital, where a total of 30 echocardiography videos were successfully obtained. Of these, 30 videos were used as the main dataset for this study. The dataset comprises 15 videos depicting normal heart conditions and 15 videos showing abnormal heart conditions.

### 4.2 Input Layer

The portable ultrasound device is equipped with a built-in application that can be downloaded from the Google Play Store or App Store and installed on any compatible device. Through this application, users can enter the patient's name, capture echocardiography images, and save the video results directly to the device's storage directory. The echocardiography images are obtained by positioning the probe of the portable ultrasound at specific points to capture the left ventricle images according to the desired view. The echocardiography images are shown in Figure 2.

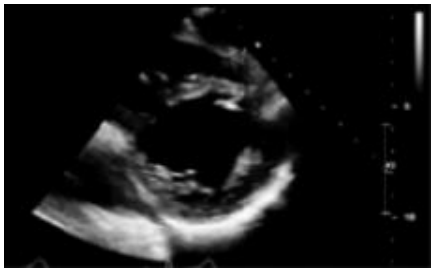

**Figure 2.** Echocardiography Image

### 4.3 Application Layer

The mobile application acts as a gateway for sending and receiving data to and from the cloud server. Echocardiography videos stored on the device's internal storage can be loaded through this application. A dedicated button is used to transfer the video data to the cloud server, where it will be processed using a previously created API. The workflow of the developed application is illustrated in Figure 3, which shows the flow chart of the mobile application.

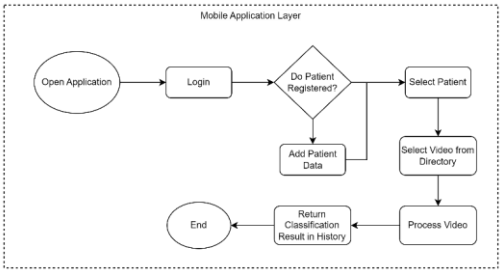


**Figure 3.** Flow chart mobile application

### 4.3 Cloud Layer

The patient's echocardiography video sent via the mobile application is processed by a detection system hosted on a cloud server (cloud-based application). This detection system is built using the Python programming language and incorporates several libraries essential for various functions: Flask for web server capabilities, OpenCV and NumPy for image processing, and Scikit-learn for machine learning. The detection system is organized into the following stages:

#### 4.3.1 Preprocessing

Image preprocessing is employed to enhance image quality before proceeding to the subsequent analysis stages. For echocardiography images, the preprocessing steps include reducing speckle noise using a median filter (1) and enhancing the image with the high-boost filter method (2 - 4). This process also involves binarizing the image to black and white (5) to facilitate further analysis [16], [17].

$$\hat{f}(x,y) = \underset{(s,t)\in S_{xy}}{median}\{g(s,t)\} \tag{1}$$

$$G_{(m,n)} = A.F_{(m,n)} - lowpass(F_{(m,n)}) \quad (2)$$

$$G_{(m,n)} = (A-1).F_{(m,n)} + [F_{(m,n)} - lowpass(F_{(m,n)})] \quad (3)$$

$$G_{(m,n)} = (A-1).F_{(m,n)} + highpass(F_{(m,n)}) \quad (4)$$

$$p(x,y) = \left\{ \frac{0,\ p(x,y) < th}{1,\ p(x,y) \geq th} \right\} \quad (5)$$

### 4.3.2 Segmentation

Image segmentation aims to simplify the image into a more meaningful form, making the analysis process easier. The Region of Interest (ROI) in echocardiography images, after preprocessing and initial segmentation using thresholding, becomes more distinct. The initial segmentation stage uses the Canny method to detect the edge lines of the heart cavity. However, the Canny filter often struggles to provide the desired contours due to small noise in certain areas. Several studies [7], [18] employ region filters to eliminate small, irrelevant contours outside the specified area. The results from the region filter are further refined by removing larger noise in the contour area using the collinear method [19]. The collinear method operates by finding the centroid of all contours, as described by Equation (6).

$$C = \left\{ \frac{\sum_{k=1}^{n} Xk}{n}, \frac{\sum_{k=1}^{n} Yk}{n} \right\} \quad (6)$$

Collinear equations are applied to calculate the slope and intercept by evaluating the distance from the center point of the cavity contour to the center points of each individual contour [10]. The collinear equations used are represented by Equations (7 - 9).

$$y = wx + b \quad (7)$$

Where *w* and *b* can be expressed by the equation:

$$w = \frac{n\sum xy - \sum x \sum y}{n\sum x^2 - (\sum x)^2} \quad (8)$$

$$b = \bar{y} - w\bar{x} \quad (9)$$

The triangle equation method (10 – 11) is employed to connect open contours of an object in an image by forming triangles with contour points. This method reconnects contour points with the smallest angles, which were previously unconnected, using the triangle equation [7]. The triangle equation is shown at Figure 4.

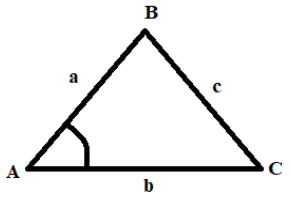


**Figure 4.** Triangle equation

$$a^2 = b^2 + c^2 - 2bc(\cos A) \quad (10)$$

$$A = acos((b^2 + c^2 - a^2) / 2bc) \quad (11)$$

### 4.3.3 Tracking

Tracking within the heart cavity is accomplished using prominent features derived from the heart cavity contours. To search for the left ventricle in the PSAX view, the number of contour coordinates is divided by the optimal feature point to be established. These prominent features are utilized to track movement across each frame using optical flow. The Lucas-Kanade method is used for this purpose, which assumes that the image displacement between two adjacent frames is small and approximately constant within the neighborhood of a point [20]. Consequently, the optical flow equation can be applied to all pixels in the image centered at point *p* [21], [22]. Therefore, the local image flow vector $(V_{x,}V_y)$ must satisfy the following equation (12):

$$\begin{aligned} &I_x(q_1)V_x + I_y(q_1)V_y = -I_t(q_1) \\ &I_x(q_2)V_x + I_y(q_2)V_y = -I_t(q_2) \\ &. \\ &. \\ &I_x(q_n)V_x + I_y(q_n)V_y = -I_t(q_n) \end{aligned} \quad (12)$$

Where $q_{1,}q_{2,\ldots\ldots,}q_{n,}$ are the pixels in the image, and $I_x(q_i), I_y(q_i), I_t(q_i)$ is a partial derivative of the image $I$ in connection with the position *x, y* and *t,* evaluation is carried out at the point $q_i$ and at this point. This equation (13) can be written in matrix form $A\upsilon = b$, where:

$$A = \begin{bmatrix} I_x(q_1) & I_y(q_1) \\ I_x(q_2) & I_y(q_2) \\ . & . \\ . & . \\ I_x(q_n) & I_y(q_n) \end{bmatrix} \qquad \upsilon = \begin{bmatrix} V_x \\ V_y \end{bmatrix} \qquad b = \begin{bmatrix} -I_t(q_1) \\ -I_t(q_2) \\ . \\ . \\ -I_t(q_n) \end{bmatrix} \quad (13)$$

The Lucas – Kanade method provides a solution by the principle of least squares, namely, by solving a 2 × 2 system.

$$A^T A\upsilon = A^T b \tag{14}$$

Where $A^T$ is the transpose of the matrix $A$, so that it can be calculated by equation (14).

$$\begin{bmatrix} V_x \\ V_y \end{bmatrix} = \begin{bmatrix} \Sigma_i I_x(q_i)^2 & \Sigma_i I_x(q_i) I_y(q_i) \\ \Sigma_i I_y(q_i) I_x(q_i) & \Sigma_i I_y(q_i)^2 \end{bmatrix}^{-1} \begin{bmatrix} -\Sigma_i I_x(q_i) I_t(q_i) \\ -\Sigma_i I_y(q_i) I_t(q_i) \end{bmatrix} \tag{15}$$

Where the central matrix in the equation (15) is the inverse matrix. The sum runs from *i = 1* to *n*. Matrix $A^T A$ often called the image structure tensor at point *p*.

### 4.3.4 Feature Extraction & Classification

Tracking the left ventricle using the optical flow method allows for the extraction of direction and distance features of movement from key points. To obtain direction features, three points (A, B, and C) are used, with point A as the origin. Point A helps determine the direction of movement towards point B. Point C is defined as the midpoint of an object connected to point A, ensuring that the tracking results for the direction of movement at point B are not influenced by the slope. This setup ensures accurate tracking of the moving point's direction [8][23].

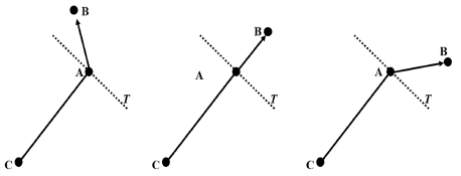


**Figure 5.** Negative value feature direction

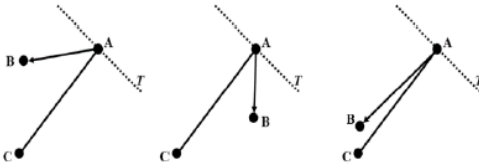


**Figure 6.** Positive value feature direction

The T line acts as a boundary that determines whether point B has a positive or negative value. Point B will be considered positive if it falls within the T line limits, corresponding to angles from 0 to 180 degrees relative to the T line. The positive value feature direction is shown at Figure 6. Conversely, point B will be assigned a negative value if it falls outside the T line limits, corresponding to angles from 181 to 360 degrees relative to the T line. The negative value feature direction is shown at Figure 5. Then, to determine the direction of movement from this point, the following trigonometric equation (16) can be used:

$$cosA = \frac{b^2+c^2-a^2}{2bc} \tag{16}$$

Euclidean distance is a mathematical concept used to measure the straight-line distance between two points in Euclidean space. It is also known as Pythagorean distance because it can be derived from the coordinates of the points using the Pythagorean theorem. In a two-dimensional plane, if two points have coordinates ($x_1$, $y_1$) and ($x_2$, $y_2$) the Euclidean distance ($d$) between these two points can be calculated using the equation (17):

$$d = \sqrt{[(x_2 - x_1)^2 + (y_2 - y_1)^2]} \tag{17}$$

This study employs the Support Vector Machine (SVM) classification algorithm, which seeks to find the optimal hyperplane in the feature space [24], [25]. In a multidimensional space, this hyperplane is a line or surface that separates the data into distinct classes, with each class positioned on either side of the hyperplane. The goal of the SVM algorithm is to maximize the margin between the two classes, ensuring the best possible separation.

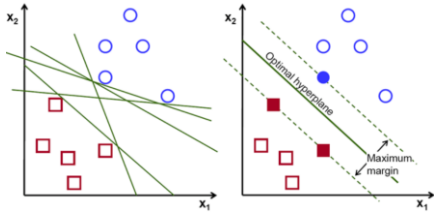


**Figure 7.** Support vector machine

The distribution of red and blue dots represents data samples, each associated with a specific class based on feature values. In the example illustrated in Figure 7, the hyperplane that separates these classes can be defined using a straight-line equation, as shown in Equation (18),

$$y = mx + c \tag{18}$$

Where y is the line function, $x$ is the data feature value, $m$ is the gradient coefficient of the line, and is the *y-intercept* of the line. The general equation of the hyperplane is as follows:

$$w^T x = 0 \tag{19}$$

Equation (19) can be represented as where $w$ and $x$ are vectors and $w^T x$ represents the point of two vectors. vector $w$ often referred to as the weight vector. Consider the equation (20-21) of a line as $y - mx - c = 0$ in this case,

$$w = \begin{Bmatrix} -c \\ -m \\ 1 \end{Bmatrix} \text{ dan } x = \begin{Bmatrix} 1 \\ x \\ y \end{Bmatrix} \tag{20}$$

$$w^T x = -c \times 1 - m \times x + y = y - mx - c = 0 \tag{21}$$

However, in practice, datasets are often not linearly separable. To address non-linear data problems, a non-linear kernel approach can be employed. Table 1 presents the mathematical equations for the most commonly used kernels in classification algorithms with the SVM method.

**Table 1.** SVM kernel

| No | Wall Movemet | Mathematical Equation |
|---|---|---|
| 1 | Linear | $k(x_1, x_2) = x_1.x_2$ |
| 2 | Sigmoid | $k(x_1, x_2) = \tanh(\gamma x_1.x_2 + c)$ |
| 3 | Polynomial | $k(x_1, x_2) = \tanh(\gamma x_1.x_2 + c)^d$ |
| 4 | RBF | $k(x_1, x_2) = \exp\left(-\gamma \left\|x_1 - x_2\right\|^2\right)$ |

### 4.4 System Deployment

Once the detection system is built, the next step is to deploy it to the cloud server. We use Amazon Elastic Compute Cloud (EC2) from Amazon Web Services (AWS) for this purpose. AWS EC2 provides Infrastructure as a Service (IaaS) that allows users to perform web-scale computing on Amazon's cloud infrastructure. The application will be deployed as an API on the web application, enabling the mobile app to interact with the API for tasks such as account login/registration, CRUD operations, and detection features. For database management, AWS offers Amazon Relational Database Service (RDS), a SQL relational database service. The web application connects to the database by initializing host, port, user, and database password in the environment variables. Additionally, Amazon Simple Storage Service (S3) will be used for storing input video files for processing and video tracking results. The diagram below illustrates the architecture system deployed on Amazon Web Services. The diagram cloud system is shown at Figure 8.

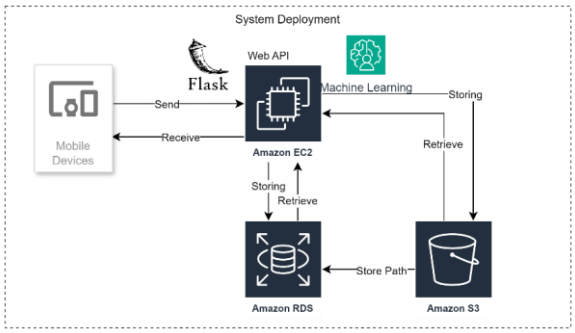


**Figure 8.** Diagram cloud system

## 5. EXPERIMENT AND ANALYSIS

This section on experiment and analysis will detail the testing and evaluation stages based on the results obtained. The goal is to assess the success level of the system. The system was developed and implemented on a PC. Testing was conducted with consideration of the components used in the

system's development. The hardware and software specifications used in the system are summarized in Table 2.

**Table 2.** Test device specification

| No | Description | Specification |
|---|---|---|
| 1 | Processor | Intel(R) Core(TM) i3-5005U CPU @ 2.00GHz (4 CPUs) |
| 2 | Memory | 8GB RAM |
| 3 | GPU | Intel(R) HD Graphics 5500 |
| 4 | *System Operation* | Windows 10 Pro 64-bit |
| 5 | *Software Build* | Visual Studio Code |
| 6 | Library | OpenCV-python 4.1.8, Flask, ScikitLearn, |
| 7 | Hardware | SonoStar UProbe C4PL Pocket Ultrasound |
| 8 | Mobile Device | Samsung Galaxy Tab A (SM T295) |
| 9 | Mobile Application *Frame*work | Flutter 3.13 |
| 10 | *Cloud Instance* | Amazon EC2 C5.large Instance |
| | | 2 VCPU, 4GB Memory |
| | | Linux Ubuntu Server 24.00 |
| 11 | Database | Amazon RDS MySQL |
| 12 | Object Storage | Amazon S3 |

## 5.2 Aplication User Interface

The application interface is designed to streamline the process for doctors. It allows doctors to authenticate using a registered account. After logging in, doctors can access and view patient data by pressing the arrow icon button. The login and patient user interface are shown at Figure 9. On the main page, doctors have the option to initiate heart examination by detecting echocardiography videos of the heart through the 'Check' button on the patient data card. This design enhances the efficiency of managing patient data and performing heart examinations, making the process quicker and more convenient for doctors.

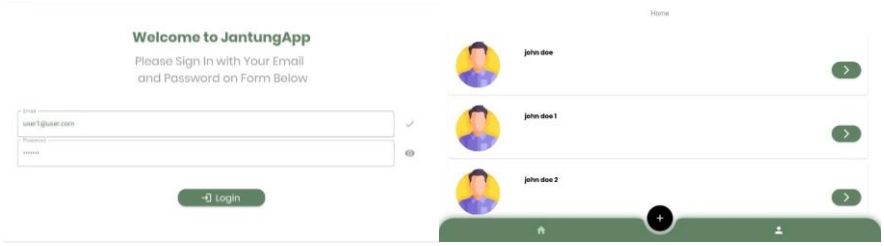


**Figure 9.** Login and patient user interface

After selecting the echocardiography video captured with a portable ultrasound, the doctor can upload the video to the server for further processing. By pressing the 'Yes' button, the application will interact with the video detection API, sending the video to the cloud server for analysis. The heart examination user interface is shown at Figure 10. The server will process the video and return the detection results, which are then displayed in the

check result table within the application. This allows the doctor to view and analyze the results directly from the application.

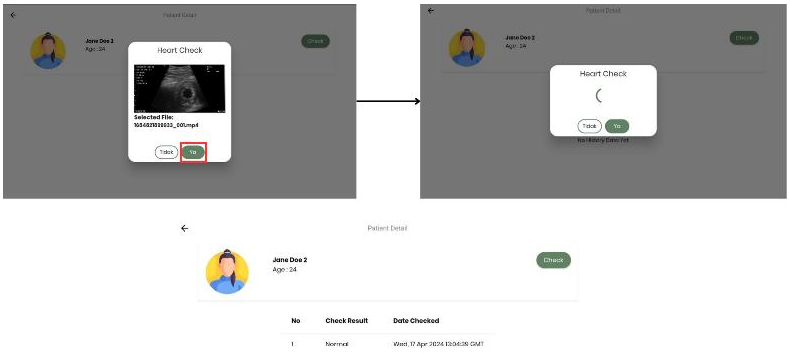


**Figure 10.** Heart examination user interface

## 5.3 Cloud Layer Application

In the cloud layer, the detection system is designed to oversee every stage of processing, including preprocessing, segmentation, tracking, and classification. This setup is essential for evaluating the results of model training within the cloud-based application. The echocardiography video sent via the mobile application will be processed by this detection system on the cloud server, ensuring that the entire workflow—from preprocessing through to classification—operates seamlessly within the cloud environment.

### 5.2.1 Preprocessing

The image preprocessing stage in echocardiography aims to enhance image quality and clarify the edges of the heart cavity are shown at Figure 11. This involves several steps: first, a median filter is applied to remove speckle noise and improve the clarity of the heart wall. Following this, a high-boost filter is used to enhance the brightness and contrast of the image. The expected result is an echocardiography image with a clear distinction between the heart wall and the left ventricle, while minimizing noise and improving overall image quality.

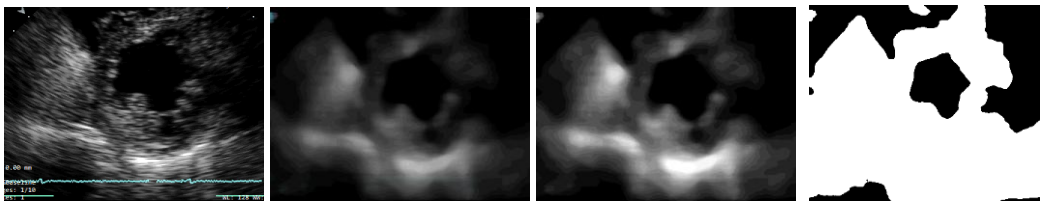

**Figure 11.** Image preprocessing

### 5.2.2 Segmentation

The segmentation process is designed to isolate the left ventricle from the heart wall shown at Figure 12. It begins with global thresholding to convert the image into a binary format, followed by edge detection using the Canny

method. However, this method often fails to fully separate the left ventricle from the surrounding structures, necessitating the use of a region filter to eliminate small contours that are deemed noise. Despite this, the region filter may not effectively remove larger noise surrounding the heart cavity. To address this issue, the collinear method is employed with an initialization point at the cavity's center to more accurately remove large noise. This is followed by the triangle equation method to close any open sections in the cavity, ensuring a complete and accurate segmentation of the left ventricle.

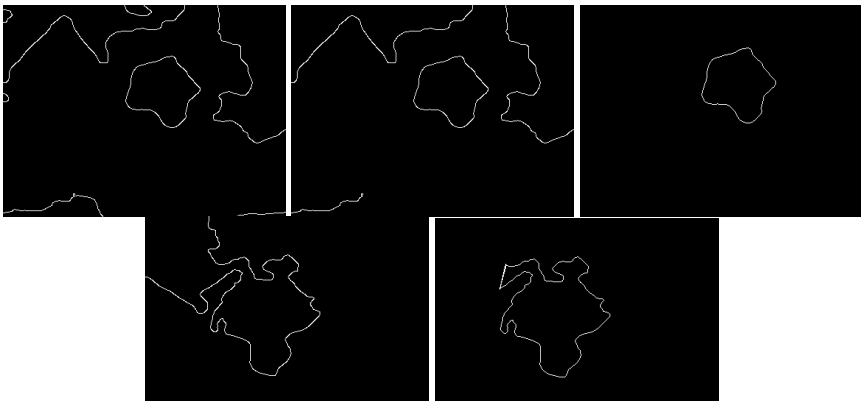

**Figure 12.** Image segmentation

### 5.2.3 Tracking

The contour of the left ventricular cavity obtained from the segmentation method serves as a valuable feature for optical flow analysis. However, not all contour lines are used for tracking in subsequent frames. This study introduces a method to identify the contour initialization point, which is a significant feature for tracking the movement of the heart wall using optical flow. This process involves selecting specific points from the edge detection results of the left ventricular cavity, ensuring that the tracking is focused on the most relevant and accurate features. The cardiac cavity tracking are shown at Figure 13.

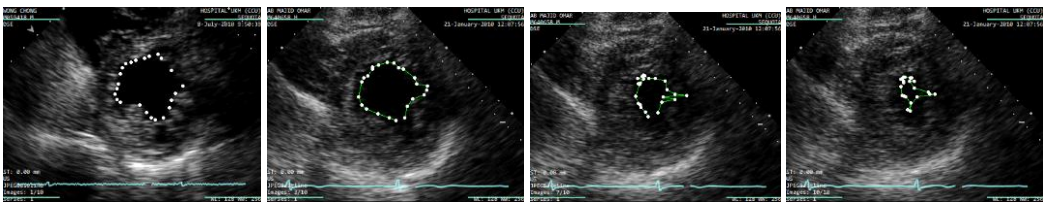

**Figure 13.** Cardiac cavity tracking

### 5.2.4 Feature Extraction and Classification

Normal hearts exhibit significant and rapid movements, while abnormal hearts display smaller and slower movements from diastole to systole. The key feature for classifying heart conditions is the direction of movement of significant features from one frame to the next, categorized into positive (indicating inward movement towards the center of the left ventricle) and

negative (indicating outward movement away from the center of the left ventricle). For each dataset, 48 features are generated from 24 extracted good features, with odd-numbered features representing inward movement and even-numbered features representing outward movement. To determine the direction of movement, a trigonometric equation calculates the angle of the shadow triangle formed between the heart's center, the initial point of the good features, and their movement point. An angle greater than 90º indicates outward movement, while an angle less than 90º indicates inward movement. This analysis continues through all frames, recording each feature's movement direction to identify the predominant feature.

**Table 4.** Good feature

| No | Good Features | Features | Value |
|---|---|---|---|
| 1 | 1 | Direction + | 0.8888 |
| 2 | | Direction – | 0.1111 |
| ... | | | |
| 47 | 24 | Direction + | 0.7777 |
| 48 | | Direction – | 0.3333 |

The next stage involves training the data to develop a model capable of classifying echocardiography images into two categories: normal or abnormal. The dataset comprises 30 images, split evenly with 15 normal and 15 abnormal heart echocardiography images. The training utilizes a Support Vector Machine (SVM) model with a 'linear' kernel and 'auto' gamma, and 20% of the dataset is reserved for testing. The results of the training are illustrated in Figure 14. The classification report indicates that the model achieved an overall accuracy of 83%, meaning 83% of the predictions were correct. For class 0, the model demonstrates a precision of 0.8, a recall of 1.0, and an F1-score of 0.89, reflecting its strong ability to identify all examples of class 0 accurately. In contrast, for class 1, while precision is perfect at 1.0, the recall is only 0.5, resulting in an F1-score of 0.67. The average macro precision and recall are 0.9 and 0.75, respectively, with an F1-score of 0.78.

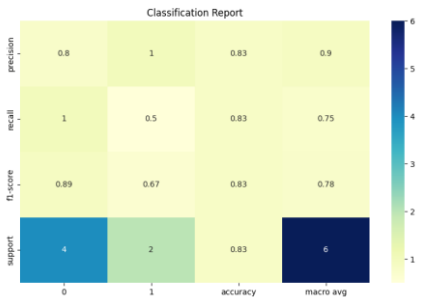


**Figure 14.** Heat map classification report

Further evaluation of the model using cross-validation revealed an average accuracy of 86.67%, with precision and recall both at 86.7%. The standard deviation of accuracy is 0.09, or 9%. While the model demonstrates strong overall performance, there remains room for improvement,

particularly in enhancing the identification of class 1 (normal). The model evaluation is shown in Figure 15.

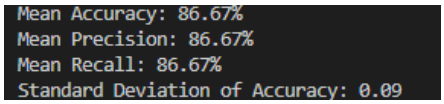


**Figure 15.** Model evaluation

## 6. CONCLUSION

Based on the testing and analysis results, the development of the Android mobile application has been successfully completed. The preprocessing stage effectively reduces noise and enhances the image quality of the left ventricle of the heart. The segmentation stage accurately produces contours and addresses open contours in some images. Tracking successfully detects contour features across frames, with normalization applied to address outliers. Feature extraction provides a good representation of the left ventricle's movement, and the SVM classification system achieves an accuracy of approximately 86%. However, there are limitations in the variety of data, particularly for the normal heart class. The cloud-based detection system, implemented using AWS services, has been successfully deployed, with computing performed on EC2 virtual machines and data storage managed through RDS and S3. Despite these accomplishments, there are areas for improvement, particularly in increasing data variety to enhance classification accuracy.

## ACKNOWLEDGMENT

We would like to thank the Academic Director of Vocational Higher Education and Electronics Engineering Polytechnic Institute of Surabaya through the Directorate of Research and Community Service. We also would like to extend our sincere thanks to the researchers at the Signal, Vision, and Graphics Laboratory, Electronics Engineering Polytechnic Institute of Surabaya.

## REFERENCES

[1] M. Lindstrom *et al.*, **Global Burden of Cardiovascular Diseases and Risks Collaboration, 1990-2021**, *J Am Coll Cardiol*, vol. 80, no. 25, 2022, doi: 10.1016/j.jacc.2022.11.001.

[2] S. Fitzsimons and R. N. Doughty, **Role of transthoracic echocardiogram in acute heart failure**, 2021. doi: 10.31083/J.RCM2203081.

[3] A. Anwar, R. Sigit, A. Basuki, I. P. Adi, and S. Gunawan, **Automatic Segmentation of Heart Cavity in Echocardiography Images : Two & Four-Chamber View Using Iterative Process Method**, *Proceedings - International Electronics Symposium on Knowledge Creation and Intelligent Computing, IES-KCIC 2019*, pp. 177–182, 2019.

[4] Y. D. Putra, R. Sigit, and H. Yuniarti, **Portable Device-Based Medical Service System for DICOM to PNG Conversion**, in *International*

*Electronics Symposium 2021: Wireless Technologies and Intelligent Systems for Better Human Lives, IES 2021 - Proceedings*, 2021. doi: 10.1109/IES53407.2021.9593962.

[5] A. Moradkhani, A. Broumandnia, and S. J. Mirabedini, **A portable medical device for detecting diseases using Probabilistic Neural Network**, *Biomed Signal Process Control*, vol. 71, 2022, doi: 10.1016/j.bspc.2021.103142.

[6] Y. Hornych, J. C. Toledo, B. Wang, W. J. Yi, and J. Saniie, **Near-Ultrasonic Communications for IoT Applications using Android Smartphone**, in *IEEE International Conference on Electro Information Technology*, 2020. doi: 10.1109/EIT48999.2020.9208265.

[7] A. S. Aziz, R. Sigit, A. Basuki, and T. Hidayat, **Cardiac motions classification on sequential PSAX echocardiogram**, *Indonesian Journal of Electrical Engineering and Computer Science*, vol. 12, no. 3, pp. 1289–1296, 2018, doi: 10.11591/ijeecs.v12.i3.pp1289-1296.

[8] R. Sigit, A. Basuki, and Anwar, **A new feature extraction method for classifying heart wall from left ventricle cavity**, *Int J Adv Sci Eng Inf Technol*, 2020, doi: 10.18517/ijaseit.10.3.12152.

[9] B. Berisha, E. Mëziu, and I. Shabani, **Big data analytics in Cloud computing: an overview**, *Journal of Cloud Computing*, vol. 11, no. 1, 2022, doi: 10.1186/s13677-022-00301-w.

[10] T. Aniamarta, A. Salsabilla Huda, and F. Lizariani Aqsha, **Causes and Treatments of Heart Attack**, *BIOLOGICA SAMUDRA*, vol. 4, no. 1, 2022, doi: 10.33059/jbs.v4i1.3925.

[11] J. Zhou, M. Du, S. Chang, and Z. Chen, **Artificial intelligence in echocardiography: detection, functional evaluation, and disease diagnosis**, 2021. doi: 10.1186/s12947-021-00261-2.

[12] Y. Muhammad, M. Tahir, M. Hayat, and K. T. Chong, **Early and accurate detection and diagnosis of heart disease using intelligent computational model**, *Sci Rep*, vol. 10, no. 1, 2020, doi: 10.1038/s41598-020-76635-9.

[13] D. Wang *et al.*, **Cloud based services for biomedical image analysis**, in *CLOSER 2013 - Proceedings of the 3rd International Conference on Cloud Computing and Services Science*, 2013. doi: 10.5220/0004370003500357.

[14] L. Liu *et al.*, **iMAGE cloud: medical image processing as a service for regional healthcare in a hybrid cloud environment**, *Environ Health Prev Med*, vol. 21, no. 6, 2016, doi: 10.1007/s12199-016-0582-7.

[15] F. Fahmi, T. H. Nasution, and Anggreiny, **Smart cloud system with image processing server in diagnosing brain diseases dedicated for hospitals with limited resources**, *Technology and Health Care*, vol. 25, no. 3, 2017, doi: 10.3233/THC-171298.

[16] I. Putu Adi Surya Gunawan, R. Sigit, and A. I. Gunawan, **Veins projection performance based on ultrasonic distance sensor in various surface**

**objects**, *Indonesian Journal of Electrical Engineering and Computer Science*, 2019, doi: 10.11591/ijeecs.v17.i3.pp1362-1370.

[17] I. Putu Adi Surya Gunawan, R. Sigit, and A. I. Gunawan, **Veins projection performance based on ultrasonic distance sensor in various surface objects**, *Indonesian Journal of Electrical Engineering and Computer Science*, 2019, doi: 10.11591/ijeecs.v17.i3.pp1362-1370.

[18] C. Nofindarwati, R. Sigit, and T. Harsono, **Detection of Heart Condition based on Echocardiography Image using Ultrasound**, *IES 2019 - International Electronics Symposium: The Role of Techno-Intelligence in Creating an Open Energy System Towards Energy Democracy, Proceedings*, pp. 522–526, 2019, doi: 10.1109/ELECSYM.2019.8901556.

[19] K. R. Ummah, R. Sigit, H. Yuniarti, and A. Anwar, **Tracking Multidimensional Echocardiographic Image using Optical Flow**, in *IES 2020 - International Electronics Symposium: The Role of Autonomous and Intelligent Systems for Human Life and Comfort*, 2020, pp. 527–533. doi: 10.1109/IES50839.2020.9231920.

[20] M. W. Asyhari, R. Sigit, B. S. B. Dewantara, and Anwar, **Comparison of Optical Flow Methods: Study about Left Ventricular Tracking in Multi View Echocardiographic Images**, in *International Electronics Symposium 2021: Wireless Technologies and Intelligent Systems for Better Human Lives, IES 2021 - Proceedings*, 2021, pp. 137–143. doi: 10.1109/IES53407.2021.9593990.

[21] **Introduction to Motion Estimation with Optical Flow**. https://adacenter.org/sites/default/files/milspec/opticalflow-overview-nanonetsdotcom.pdf

[22] D. N. Z. A. Jesemi, H. Ujir, I. Hipiny, and S. F. S. Juan, **The analysis of facial feature deformation using optical flow algorithm**, *Indonesian Journal of Electrical Engineering and Computer Science*, vol. 15, no. 2, pp. 769–777, 2019, doi: 10.11591/ijeecs.v15.i2.pp769-777.

[23] R. Sigit, T. Karlita, T. Hidayat, and Anwar, **Left Ventricular Movement Feature Extraction: A New Method for Classifying Heart Condition in Four-Chamber and Two-Chamber Views**, *International Journal of Intelligent Engineering and Systems*, vol. 15, no. 4, pp. 292–302, 2022, doi: 10.22266/ijies2022.0831.27.

[24] O. Natan, A. I. Gunawan, and B. S. B. Dewantara, **Grid SVM: Aplikasi Machine Learning dalam Pengolahan Data Akuakultur**, *Jurnal Rekayasa Elektrika*, 2019, doi: 10.17529/jre.v15i1.13298.

[25] K. Shreedarshan and S. Sethu Selvi, **Crowd recognition system based on optical flow along with SVM classifier**, *International Journal of Electrical and Computer Engineering*, vol. 9, no. 4, pp. 2451–2459, 2019, doi: 10.11591/ijece.v9i4.pp2451-2459.